JOC The Journal of Organic Chemistry

Article

pubs.acs.org/joc

Calix[2]thia[4]phyrin: An Expanded Calixphyrin with Aggregation-Induced Enhanced Emission and Anion Receptor Properties

Ganesan Karthik, Pallavee Vitti Krushna, A. Srinivasan, and Tavarekere K. Chandrashekar*

School of Chemical Sciences, National Institute of Science Education and Research (NISER), IOP campus, Sainik School – PO, Bhubaneshwar 751005, Odisha, India

Supporting Information

ABSTRACT: The synthesis of calix[2]thia[4]phyrin **3**, a core-modified expanded calixphyrin, by an efficient synthetic route is reported. **3** exhibits an aggregation-induced enhanced emission (AIEE) phenomenon upon addition of increasing amounts of water. This is attributed to the restricted intramolecular rotation of the *meso*-aryl rings present on the sp^3 bridging carbons. SEM studies revealed the formation of aggregation in an acetonitrile/water mixture with an average diameter of the aggregate in the range 0.38–2.08 μm. The photoluminescence quantum yield of **3** in 9:1 water/acetonitrile is 5-fold higher than the quantum yield in acetonitrile alone. Single-crystal X-ray analysis of **3** revealed a chairlike conformation stabilized by N–H···N and C–H···π intramolecular hydrogen-bonding interactions. Fluorine atoms on the *meso*-pentafluorophenyl groups are involved in C–H···F intermolecular hydrogen-bonding interactions to generate a two-dimensional supramolecular assembly in the solid state. In the diprotonated state, **3** has affinity for anions and forms 1:1 complexes with SO_4^{2-}, NO_3^-, Cl^-, and ClO_4^- in solution. The tetrahedral anions bind more strongly than the other anions. Single-crystal X-ray structure studies of the ClO_4^- anion complex with **3** revealed the formation of both 1:1 and 1:2 complexes in the solid state, with the host and the guest being held together by N–H···O hydrogen-bonding interactions.

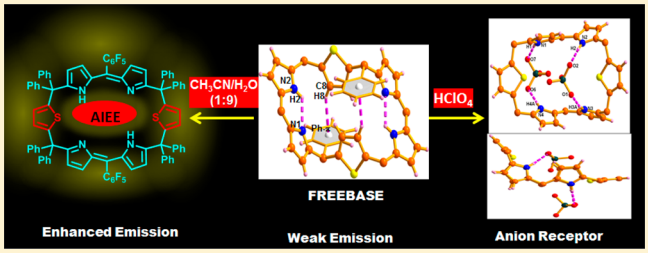

INTRODUCTION

Calixphyrins, a hybrid of calixpyrroles and porphyrins, have received attention in recent years because of their conformational flexibility to adopt various nonplanar conformations.[1] The conformations depend on the number of pyrrole rings and nature of their linkage in a cyclic structure.[2] Structurally, they contain both sp^2- and sp^3-hybridized *meso* carbon links that connect the pyrrole rings (Chart 1). The presence of sp^3-hybridized *meso* carbon centers disrupts the π conjugation and allows the macrocycle to adopt a nonplanar conformation.[3,4] Since they have properties analogous to both porphyrins and calixpyrroles, they have found applications as metal ion receptors[5] anion-complexing agents[6] and exhibit rich coordination chemistry.[7] Even though calixphyrins have been synthesized by various research groups in decent yields,[1−4,8] general synthetic protocols for the syntheses of calixphyrins with one, two (**A**), and three sp^3-hybridized *meso* carbons were reported by Sessler and co-workers,[9,10] and all of the structures of the macrocycles were confirmed by single-crystal X-ray structure analyses. To date, series of expanded calixphyrins containing five to 28 pyrrole rings have been reported in the literature.[8d] In particular, calix[6]phyrin (**B**), which is more relevant to this manuscript, binds strongly with anions.[4] The N-confused calix[6]phyrins reported by Furuta and co-workers selectively coordinate with salts of group-8 metal ions, specifically Pt(II).[11] The metal complexes exhibit an intense emission in the near-IR region. Recently, series of calixphyrins and expanded calixphyrins were reported by several groups, and their rich host–guest chemistry has been explored using various anions and cations.[5−7,12]

Chart 1. Structures of Various Calixphyrins

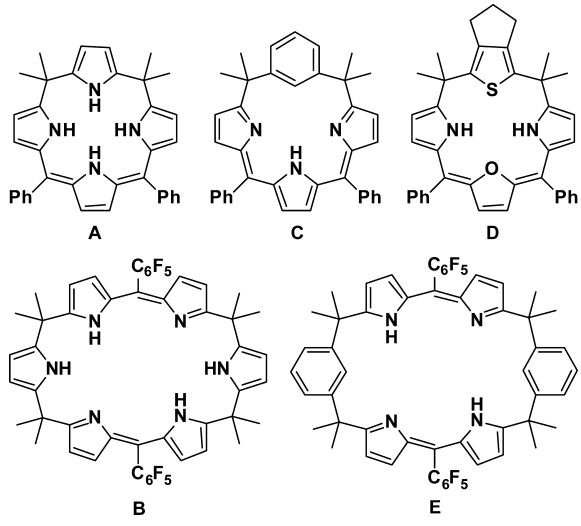

Received: June 7, 2013
Published: August 13, 2013

   dx.doi.org/10.1021/jo401232a | J. Org. Chem. 2013, 78, 8496–8501

However, the synthesis of core-modified calixphyrins and their expanded derivatives is still in its infancy. Latos-Grażyński and co-workers demonstrated the synthesis and coordination chemistry of porphodimethene **C** incorporating a *m*-benzene ring,[13a] and Hung and co-workers reported the binding ability of **C**, which senses Zn(II) ions exclusively.[13b,c] Matano and co-workers reported the synthesis of thiophene- and furan-containing calixphyrin **D** and its Pd complexes and also examined the catalytic activity of the respective metal complexes.[14] Recently, Srinivasan and co-workers reported the synthesis of calix[2]-*m*-benzo[4]phyrin **E**, which contains phenyl groups in the macrocycle framework. This calixphyrin exhibits aggregation-induced enhanced emission (AIEE) and acts as a Hg(II) ion sensor.[5] Latos-Grażyński and co-workers reported synthesis and characterization of calix[2]sila[4]-phyrins.[15] Herein we report a core-modified expanded calixphyrin, calix[2]thia[4]phyrin **3**, which contains two thiophene rings linked to four pyrrole units in a cyclic structure. There are four sp^3 *meso* carbon links in the structure. In solution, this calixphyrin exhibits AIEE due to the presence of restricted intramolecular rotation (IMR) attributed to the phenyl rings present on the sp^3 carbons.[16] Furthermore, **3** binds to different anions such as NO_3^-, Cl^-, SO_4^{2-}, and ClO_4^-. The X-ray structure of the ClO_4^- complex indicates that the host and anion are held together by intermolecular N–H···O hydrogen-bonding interactions.

RESULTS AND DISCUSSION

The synthesis of **3** is outlined in Scheme 1. The synthetic methodology followed is basically an acid-catalyzed condensation reaction of appropriate precursors.[4] Stirring a dichloromethane solution of bis(pyrrolyl)thiophene **1**[17] with pentafluorobenzaldehyde (**2**) in the presence of trifluoroacetic acid (TFA) followed by oxidation with 2,3-dichloro-5,6-dicyano-1,4-benzoquinone (DDQ) afforded **3** in 20% yield along with a trace amount of the higher analogue calix[3]thia[6]phyrin (see the Supporting Information). **3** is highly soluble in common organic solvents but insoluble in water.

Scheme 1. Synthesis of Calix[2]thia[4]phyrin 3

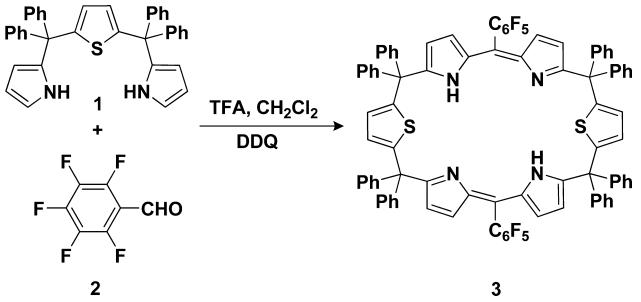

3 was fully characterized by electronic absorption, electrospray ionization mass spectrometry (ESI-MS), and nuclear magnetic resonance (NMR) spectral studies, and the structure was further confirmed by single-crystal X-ray diffraction analysis. The exact composition of **3** was established by ESI-MS, which showed a molecular ion signal at m/z 1446.3792 $[M + 2H]^+$ (see the Supporting Information).

The ^1H NMR spectrum of **3** in CD_2Cl_2 at room temperature substantiated the expected structure (see the Supporting Information). The pyrrole NH protons resonated as a broad singlet at 12.10 ppm, and the assignment was confirmed by a D_2O exchange experiment. The unusual downfield shift of the NH proton signal suggested a strong intramolecular hydrogen-bonding interaction with the imine nitrogens. The doublets at 6.30 and 5.88 ppm correspond to the four β-CH protons of the two dipyrrin rings connected through the *meso*-pentafluorophenyl-substituted methene bridge, and the assignment was confirmed by $^1H-^1H$ correlation spectroscopy (COSY) analysis. The signal due to the remaining four β-CH protons of the thiophene rings appeared as a sharp singlet at 6.42 ppm. Furthermore, relative to **1**, the downfield shift of the pyrrolic NH protons in **3** and the absence of the resonance for the two α-CH protons in the pyrrolic rings, which was observed for **1** at 6.72 ppm, clearly reflect the typical π conjugation between the amine and imine pyrrole nitrogens and the formation of the macrocycle. The *meso*-phenyl protons resonated as a multiplet at 7.15 ppm.

The electronic spectral analyses of **3** in dilute acetonitrile solution showed an absorption band at 449 nm, which is attributed to a $\pi-\pi^*$ transition of the dipyrrin moiety. Upon excitation at 449 nm, the emission spectrum in dilute acetonitrile showed a weak band at 538 nm. These results are comparable to those for similar calixphyrins that are already known in the literature.[5] We observed an anomalous behavior in the absorption and emission spectra of **3** when the percentage of water in the solvent mixture was increased. As more water was added, the absorption band at 449 nm broadened and experienced a bathochromic shift to 460 nm (see the Supporting Information). On the other hand, the weak emission band remained unchanged as the percentage of water

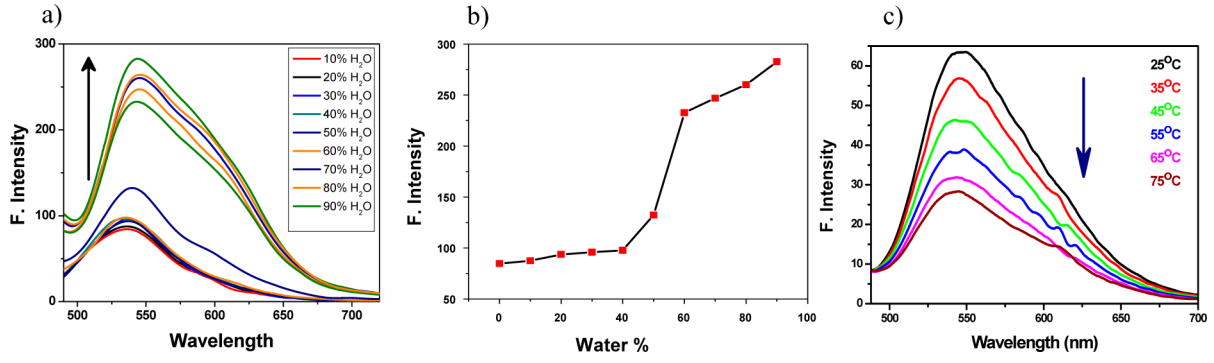

Figure 1. (a) Emission spectra of **3** in acetonitrile/water mixtures with different fractions of water (0–90 vol %) at 25 °C. (b) Variation in the emission intensity of **3** with the water content in the acetonitrile/water mixture at 25 °C. (c) Temperature effect on the emission peak intensity of **3** in 1:9 (v/v) acetonitrile/water mixture (λ_{ex} = 449 nm).

dx.doi.org/10.1021/jo401232a | J. Org. Chem. 2013, 78, 8496–8501

in the acetonitrile/water mixture increased to 50%, and as the water content increased from 50% to 90%, the emission intensity at 538 nm was enhanced (Figure 1a). These observations clearly indicate AIEE in **3**. The intensity variation suggests that **3** starts to congregate at a water fraction of 50% and that the aggregation continues to increase as the water fraction increases from 50% to 90% (Figure 1b). To have a quantitative picture of the emission enhancement upon aggregation, we estimated the photoluminescence (PL) quantum yields (Φ_F) of **3** in acetonitrile and a 1:9 (v/v) acetonitrile/water mixture and found that Φ_F of the latter (6.9×10^{-3}) is 5-fold higher than that of the former (1.38×10^{-3}). Basically, when the water content is increased to 50%, a critical point is reached, after which the addition of a small amount of water significantly promotes efficient calixphyrin self-aggregation, leading to an increase in the emission intensity.

Furthermore, the effect of temperature on the emission spectrum of **3** in the same solvent mixture (1:9 v/v) was also investigated (Figure 1c). When the temperature was lowered from 75 to 25 °C, the emission intensity at 538 nm was further enhanced as a result of the increase in aggregate formation, while raising the temperature decreased the intensity as a result of disaggregation of the molecules. These results suggest that the aggregated state of the compound at low temperature changes into a monomer-like state at high temperatures. As the temperature decreases, the thermally induced or activated intramolecular rotations of the *meso*-phenyl and *meso*-pentafluorophenyl groups are gradually restricted. Thus, reduction in thermal energy decreases the intramolecular rotation (IMR) of the *meso*-aryl groups and rigidifies the macrocycle as a whole, thereby enhancing the solution emission. Overall, the aggregates at low temperatures are more rigid and more emissive than the free monomer. Single-crystal X-ray studies of **3** further confirmed the restriction in intramolecular rotations during aggregation.

The aggregate formation of **3** was further confirmed from the microscopic analysis and dynamic light scattering (DLS) studies. The cubic-shaped aggregates were observed by scanning electron microscopy analysis, with sizes ranging from 0.38 to 2.08 μm. When different compositions of the acetonitrile/water mixture were used, nanoparticles with average diameters from 150 nm (30:70) to 122 nm (10:90) were detected in the DLS studies (see the Supporting Information). The reduction in the nanoparticle size with increasing fraction of water in the solvent mixture leads to an effective restriction in the IMR of the fluorophore, resulting in enhanced emission.

The single-crystal X-ray structure of **3** is shown in Figure 2. The molecule is located on a crystallographic twofold axis. As predicted from the spectral analysis, there are two intramolecular hydrogen-bonding interactions observed in **3**: (i) between the amine (N2−H2) and imine pyrrolic nitrogens (N1) present in the dipyrrin moieties and (ii) between thiophene ring β-CH (C8−H8) and the phenylic π cloud [Ph(π)] of one of the *meso*-phenyl units (Figure 2a). The distances and angles of the N2−H2···N1 and C8−H8···Ph(π) hydrogen-bonding interactions are 2.23 Å, 122° and 2.70 Å, 152°, respectively. The dipyrrin units are perpendicular to the *meso*-pentafluorophenyl units as well as the thiophene rings and adopt a chairlike conformation (Figure 2b). The crystal analysis of **3** revealed three types of 1D arrays through intermolecular hydrogen-bonding interactions (with distances and angles in parentheses): (i) C13−H13···F3 (2.53 Å, 171°); (ii) C19−H19···F1 (2.87 Å, 133°) and C18−H18···F4 (2.64 Å, 124°) and (iii) C38−H38···F4 (2.73 Å, 136°) (see the Supporting Information). These 1D arrays combine together to generate a 2D supramolecular assembly in the solid state (Figure 2c). Furthermore, the interplane distances (involving planes generated by the *meso*-carbon atoms, e.g., C5, C10, C15, C5′, C10′ C15′) between the two units of macrocycles (Figure 2c and the Supporting Information) range from 3.90 to 7.95 Å, which accommodate all of the aryl units together and restrict the IMR within them. Overall, both the intra- and intermolecular interactions restrict the IMR in the solid state, leading to enhanced emission as observed in the aggregated state.

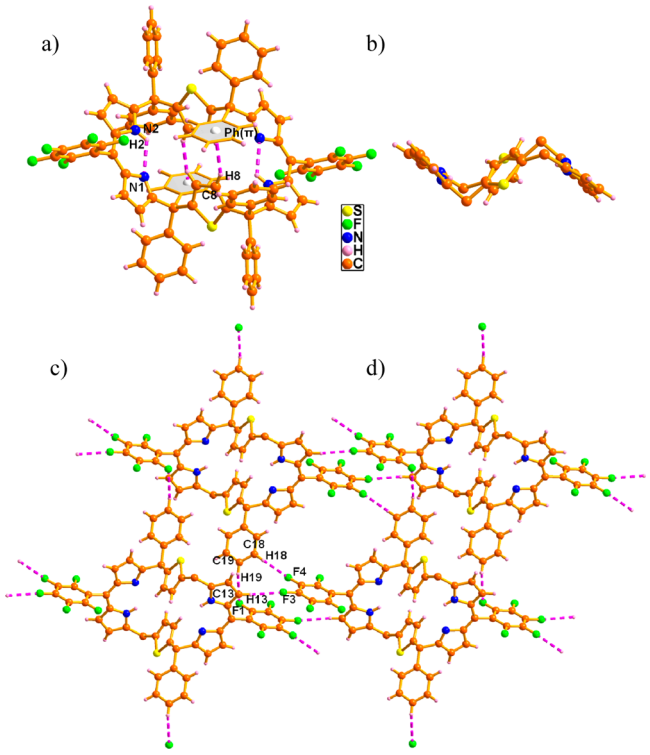

Figure 2. Single-crystal X-ray structure of **3**: (a) top view with intramolecular hydrogen-bonding interactions; (b) side view; (c) 2D array with intermolecular hydrogen-bonding interactions. The *meso*-phenyl and *meso*-pentafluorophenyl units in the side view and units that are not involved in intra- and intermolecular hydrogen-bonding interactions in the 2D array have been omitted for clarity.

The larger and flexible cavity size of **3** prompted us to explore the receptor properties of the macrocycle. The acidic nature of the calixpyrrole readily binds with various tetrabutylammonium salts;[18] however, in order to generate the calixphyrin−anion complex, in addition to the regular amine nitrogens, the imine nitrogens are also protonated to generate an efficient receptor species, which promotes not only the hydrogen-bonding interactions but also the electrostatic interactions. Therefore, protonation of the basic nitrogens in **3** leads to the formation of diprotonated species, which creates a driving force that attracts various anions toward its cavity. As discussed, **3** reported here has a $\pi-\pi^*$ absorption in the visible region, allowing us to use electronic spectra to monitor the anion complexation. The preliminary qualitative experiment was performed using a dichloromethane solution of **3** with increasing concentrations of trifluoroacetic acid. As the acid concentration was increased, the band at 449 nm gradually

dx.doi.org/10.1021/jo401232a | J. Org. Chem. 2013, 78, 8496−8501

decreased and a new band appeared at 494 nm with a bathochromic shift of 45 nm, suggesting the formation of monoprotonated species, as there are two species that exist in dynamic equilibrium. With further increases in the concentration of the acid, the band at 494 nm was further red-shifted, and the new band appeared at 506 nm (a shift of 12 nm), revealing the formation of diprotonated **3** (see the Supporting Information). When the concentration of the acid was increased further, the band was further shifted to 523 nm, which suggested the extent of binding of $CF_3CO_2^-$ ion with **3**. Overall, the preliminary binding studies revealed the formation of the mono- and diprotonated species and the binding of anion with **3**. The results encouraged us to perform binding studies of various important anions such as perchlorate, sulfate, nitrate, and chloride with a dichloromethane solution of **3** (6×10^{-6} M), and the results are presented in Table 1. In these experiments, the following observations were made:

Table 1. Absorption Maxima (λ_{max}) and Binding Constants (K) for Binding of Anions with 3 (λ_{max} = 449 nm)

entry	anion	λ_{max} (nm)	K (M^{-1})
1	chloride	517	3.78×10^2
2	nitrate	516	4.62×10^2
3	sulfate	522	5.64×10^3
4	perchlorate	523	2.50×10^4

(i) Addition of different amounts of anion (e.g., 6×10^{-4} to 6×10^{-2} M $HClO_4$) to the solution of **3** at constant concentration resulted in a decrease in the absorbance at 449 nm and the simultaneous appearance of a new band at 516−523 nm. Thus, the anion complexation effectively results in a red shift of 67−74 nm, and the magnitude of this red shift was different for different anions.[19] For example, as the concentration of perchlorate ion was increased, the band at 449 nm shifted to 523 nm and the color of the solution changed from pale yellow to pink (Figure 3a).

(ii) The isosbestic points for all of the anion complexes were observed to be between 483 and 490 nm (Figure 3a). The isosbestic point suggests the presence of equilibrium between the **3** and **3**·anion complex.

(iii) The binding constant values (calculated using the Benesi−Hildebrand equation)[20] varied from 3.78×10^2 to 2.50×10^4 M^{-1}, with ClO_4^- ion showing the strongest binding (Figure 3b). Job's plots revealed 1:1 binding between **3** and the anions (Figure 3c).

(iv) The binding constant depends on the compatibility between the sizes of the receptor cavity and the anion and the number of available hydrogen-bonding sites (involving either regular hydrogens or protonated hydrogens).[21] Comparison of the binding constants suggests that the sulfate and perchlorate anions bind more strongly than the nitrate and chloride anions. For example, the binding constant of perchlorate anion is 66-fold higher than that of chloride anion, presumably suggesting that the cavity size is more suitable for the tetrahedral anions.

The final confirmation of anion binding came from single-crystal X-ray structure analysis of calixphyrin **3**·$2H^{+2}$ complexed with perchlorate anion, which crystallized in the monoclinic system with the $P\bar{1}$ space group (Figure 4). As observed from the electronic spectral analysis, we expected a 1:1 binding mode for anions with **3**, in which all four NHs of **3** were supposed to bind with an anion. However, the crystallographic analysis showed that the unit cell contains two units of **3** with three ClO_4^- ions. The addition of excess anions during crystallization afforded both 1:1 and 1:2 binding mode in the solid state.

All of the intramolecular hydrogen bonds observed in **3** (Figure 2a) are replaced by intermolecular hydrogen bonds with ClO_4^- anions, where one of the units binds with two ClO_4^- anions in 1:2 ratio (Figure 4a,c). The pyrrole units in one of the bis(pyrrolyl)thiophene units (N1−H1 and N4−H4A) point upward and bind with O7 and O6 of one of the ClO_4^- ions with distances and angles of 2.19 Å, 163° for N1−H1···O7 and 2.06 Å, 175° for N4−N4A···O6, respectively. The pyrrole units in the second bis(pyrrolyl)thiophene unit (N2−H2 and N3−H3A) point downward and bind with the second ClO_4^- ion (O2 and O1) with distances and angles of 2.14 Å, 175° for N2−H2···O2 and 1.96 Å, 166° for N3−H3A···O1, respectively (Figure 4c). On the other hand, the second **3** unit in the unit cell binds with only one ClO_4^- ion in a 1:1 ratio (Figure 4b,d), with one set of pyrrole units bound to the third ClO_4^- ion with distances and angles of 2.01 Å, 166° for N5−H5A···O14 and 2.11 Å, 174° for N7−H7A···O15, respectively, while the second bis(pyrrolyl)thiophene unit remains empty.

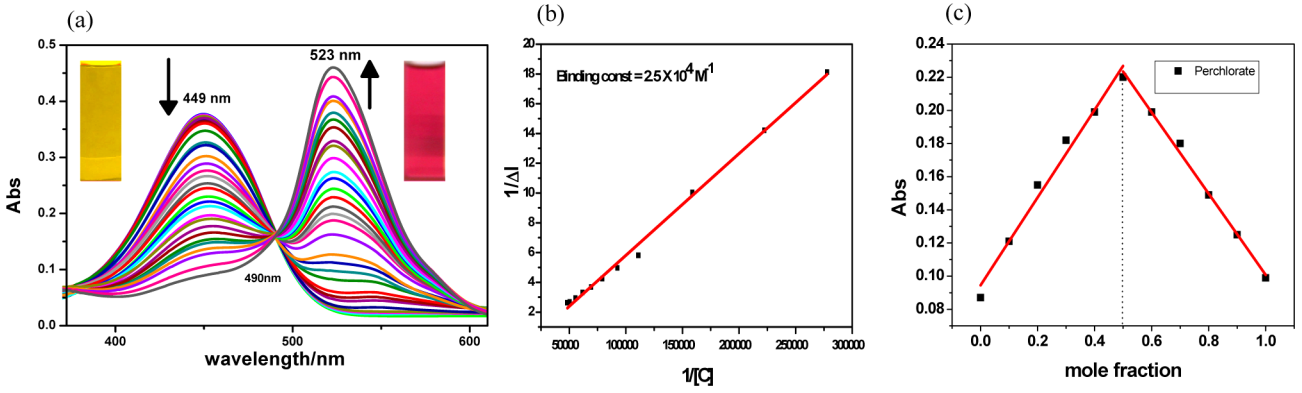

Figure 3. (a) Absorption spectra of **3** upon addition of ClO_4^- ions in CH_2Cl_2. (b) Benesi−Hildebrand plot and (c) Job's plot for the **3**·ClO_4^- system.

dx.doi.org/10.1021/jo401232a | J. Org. Chem. 2013, 78, 8496−8501

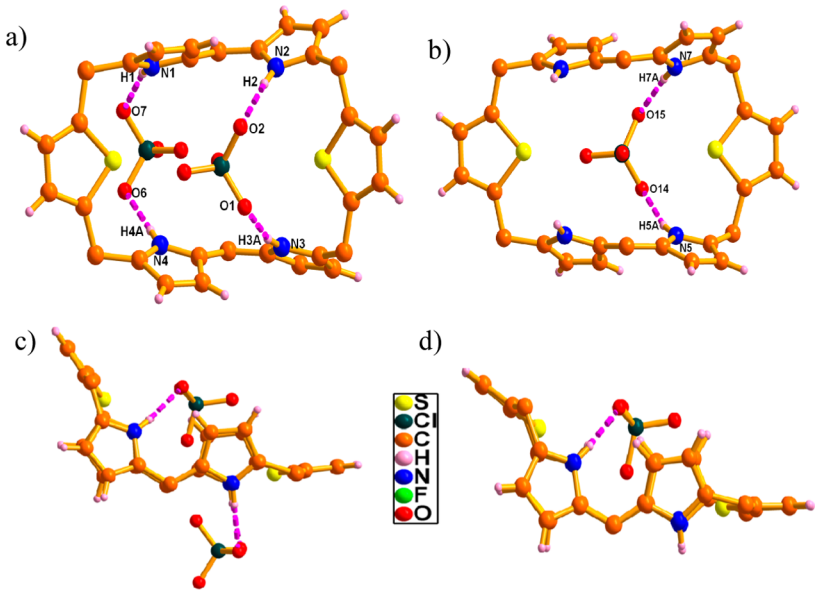

Figure 4. Single-crystal X-ray structure of **3·2H**$^{+2}$ bound with ClO_4^- anion. (a, b) Top views and (c, d) side views of (a, c) 1:2 and (b, d) 1:1 intermolecular hydrogen-bonding interactions with ClO_4^- ions. The *meso*-aryl groups have been omitted for clarity.

SUMMARY

We have successfully synthesized core-modified expanded calixphyrins by a simple synthetic strategy. The steric crowding by the phenyl substitution on the sp^3 *meso* carbons not only restricts the intramolecular rotations, inducing an AIEE effect, but also forces the macrocycle to adopt a distorted chairlike conformation in the solid state. Thus, it is possible to create strongly luminescent materials by increasing the number of sp^3 *meso* carbon bridges in the larger systems such as octa-, nona-, and decacalixphyrins. Furthermore, the anion binding properties reported here suggest that macrocycles such as **3** have a stronger affinity for tetrahedral ions. However, in order to achieve specificity and selectivity, one has to modify the macrocycle cleft and the site of anion binding by appropriate peripheral substitutions. Studies in this direction are in progress in our laboratory.

EXPERIMENTAL SECTION

All of the anhydrous solvents used for the reactions were purified by general purification procedures. The NMR spectra were recorded with a 400 MHz spectrometer in $CDCl_3$ or CD_2Cl_2 using tetramethylsilane (TMS) as an internal standard. NMR solvents were used as received. Masses of the compounds were recorded on an ESI-TOF mass spectrometer. Photophysical studies were carried out using a previously reported procedure.[5] Fluorescence quantum yields in solution were determined using fluorescein in 0.1 M NaOH (Φ_F = 0.95) as a reference. X-ray data were recorded on a single-crystal X-ray diffractometer equipped with a large-area charge-coupled device (CCD) detector. The structure was refined with the SHELX-97 programs. Single crystals of free base **3** were obtained from vapor diffusion of hexane into CH_2Cl_2, while single crystals of **3** with ClO_4^- ion were obtained from vapor diffusion of hexane into $CHCl_3$. DLS analyses were carried out at 25 °C.

Synthesis of 2,5-Bis(diphenylpyrrolylmethyl)thiophene (1). 2,5-Bis(diphenylhydroxymethyl)thiophene (1 g, 1 equiv, 2.23 mmol) was added to pyrrole (7.725 mL, 111.5 mmol) under an argon atmosphere. After 10 min, TFA (0.053 mL, 0.3 equiv, 0.69 mmol) was added, and the mixture was stirred for 30 min at ambient temperature. Dichloromethane (30 mL) and KOH (2−3 equiv) were added to quench the reaction and neutralize the acid, respectively. The organic layer was then extracted with dichloromethane and dried over anhydrous sodium sulfate. The solvent was removed by rotary evaporation. The crude product was purified by silica gel column chromatography (100−200 mesh) with 95:5 petroleum ether/ethyl acetate, affording a yellow-colored semisolid in 45% yield. ESI-MS *m*/*z*: calcd for $C_{38}H_{30}N_2S$, 546.2130; found, 546.2143. ^{1}H NMR (400 MHz, $CDCl_3$, 298 K) δ: 7.92 (s, NH, 2H), 7.28−7.09 (m, Ph, 20H), 6.58 (s, thiophene, 2H), 6.73−6.71 (q, J = 4.2 Hz, 2H), 6.15−6.13 (q, J = 4.0 Hz, 2H), 5.96−5.95 (m, 2H).

Synthesis of Calix[2]thia[4]phyrin (3). Pentafluorobenzaldehyde (0.089 g, 1 equiv, 0.46 mmol) was added to a solution of **1** (250 mg, 1 equiv, 0.46 mmol) in anhydrous dichloromethane (250 mL) under an argon atmosphere. Next, TFA (0.21 mL, 6 equiv, 0.0028 mmol) was added, and the mixture was stirred for 2 h in the dark. 2,3-Dichloro-5,6-dicyano-1,4-benzoquinone (DDQ) (0.312 g, 3 equiv, 1.37 mmol) was then added, and the reaction mixture was opened to air. The organic layer was then extracted with dichloromethane, washed with brine, and dried over anhydrous sodium sulfate. The solvent was removed using rotary evaporation, and the crude product was repeatedly purified by basic alumina column chromatography. The compound was eluted with 19:1 petroleum ether/dichloromethane, giving a yellow solid in 20% yield. Mp: 233−235 °C (decomposition). ESI-MS *m*/*z*: calcd for $[C_{90}H_{54}F_{10}N_4S_2 + 2H]^+$, 1446.3787; found, 1446.3792. Anal. Calcd for $C_{90}H_{54}F_{10}N_4S_2$: C, 74.78; H, 3.77; N, 3.88. Found: C, 74.74; H, 3.79; N 3.86. IR (CH_2Cl_2) ν_{max} (cm^{-1}): 3428, 2921, 2851, 1622, 1464, 1044. ^{1}H NMR (400 MHz, CD_2Cl_2, 298 K) δ: 12.10 (s, NH, 2H), 7.18−7.13 (m, Ph, 40H), 6.42 (s, thiophene, 4H), 6.3−6.29 (d, J = 4.4 Hz, 4H), 5.88−5.87 (d, J = 4.4 Hz, 4H). ^{13}C NMR (100 MHz, $CDCl_3$, 298 K) δ: 149.30, 146.74, 146.0, 140.80, 130.19, 130.09, 130.06, 128.52, 128.38, 128.06, 127.64, 127.51, 125.81, 122.48, 109.30, 59.41. UV/vis (CH_2Cl_2) λ_{max} [nm] (ε [10^4 M^{-1} cm^{-1}]): 449 (1.39).

ASSOCIATED CONTENT

Supporting Information

Spectral and structural characterization of all the new compounds and crystallographic data for **3** and **3·2H**$^{+2}$ (CIF). This material is available free of charge via the Internet at http://pubs.acs.org.

dx.doi.org/10.1021/jo401232a | J. Org. Chem. 2013, 78, 8496−8501

AUTHOR INFORMATION

Corresponding Author

*E-mail: tkc@niser.ac.in. Tel: (+91)674-230-4001. Fax: (+91) 674-230-2436.

Notes

The authors declare no competing financial interest.

ACKNOWLEDGMENTS

T.K.C. thanks the Department of Science and Technology (DST) (New Delhi, India) for the J. C. Bose Fellowship. We thank Dr. V. Krishnan and Dr. Arun Kumar, (SCS, NISER, Bhubaneswar) for solving the crystal structures of **3** and **3.2H**$^{+2}$ with perchlorate anion.

REFERENCES

(1) Král, V.; Sessler, J. L.; Zimmerman, R. S.; Seidel, D.; Lynch, V.; Andrioletti, B. *Angew. Chem., Int. Ed.* **2000**, *39*, 1055−1058.

(2) Sessler, J. L.; Zimmerman, R. S.; Bucher, C.; Král, V.; Andrioletti, B. *Pure. Appl. Chem.* **2001**, *73*, 1041−1057.

(3) Benech, J.-M.; Bonomo, L.; Solari, E.; Scopelliti, R.; Floriani, C. *Angew. Chem., Int. Ed.* **1999**, *38*, 1957−1959.

(4) Bucher, C.; Zimmerman, R. S.; Lynch, V.; Král, V.; Sessler, J. L. *J. Am. Chem. Soc.* **2001**, *123*, 2099−2100.

(5) Salini, P. S.; Thomas, A. P.; Sabarinathan, R.; Ramakrishnan, S.; Sreedevi, K. C. G.; Reddy, M. L. P.; Srinivasan, A. *Chem.—Eur. J.* **2011**, *17*, 6598−6601.

(6) (a) Sessler, J. L.; Camiolo, S.; Gale, P. A. *Coord. Chem. Rev.* **2003**, *240*, 7−55. (b) Dehaen, W. *Top. Heterocycl. Chem.* **2010**, *24*, 75−102. (c) Finnigan, E. M.; Giordani, S.; Senge, M. O.; McCabe, T. *J. Phys. Chem. A* **2010**, *114*, 2464−2470. (d) Jha, S. C.; Lorch, M.; Lewis, R. A.; Archibald, S. J.; Boyle, R. W. *Org. Biomol. Chem.* **2007**, *5*, 1970−1974.

(7) (a) Matano, Y.; Fujita, M.; Miyajima, T.; Imahori, H. *Organometallics.* **2009**, *28*, 6213−6217. (b) Furuta, H.; Ishizuka, T.; Osuka, A. *Inorg. Chem. Commun.* **2003**, *6*, 398−401.

(8) (a) Angelis, S. D.; Solan, E.; Floriani, C.; Villa, J. A. C.; Rizzoli, C. *J. Am. Chem. Soc.* **1994**, *116*, 5702−5713. (b) Angelis, S. D.; Solan, E.; Floriani, C.; Villa, J. A. C.; Rizzoli, C. *J. Am. Chem. Soc.* **1994**, *116*, 5691−5701. (c) Bonomo, L.; Toraman, G.; Solari, E.; Scopelliti, R.; Floriani, C. *Organometallics.* **1999**, *18*, 5198−5200. (d) Setsune, J.; Tsukajima, A.; Watanabe, J. *Tetrahedron Lett.* **2007**, *48*, 1531−1535.

(9) Bucher, C.; Seidel, D.; Lynch, V.; Král, V.; Sessler, J. L. *Org. Lett.* **2000**, *2*, 3103−3106.

(10) Bucher, L.; Zimmerman, R. S.; Lynch, V.; Sessler, J. L. *Chem. Commun.* **2003**, 1646−1647.

(11) Won, D. H.; Toganoh, M.; Terada, Y.; Fukatsu, S.; Uno, H.; Furuta, H. *Angew. Chem., Int. Ed.* **2008**, *47*, 5438−5441.

(12) Gokulnath, S.; Chandrashekar, T. K. *Org. Lett.* **2008**, *10*, 637−640.

(13) (a) Stępień, M.; Latos-Grażyński, L.; Szterenberg, L.; Panek, J.; Latajka, Z. *J. Am. Chem. Soc.* **2004**, *126*, 4566−4580. (b) Hung, C.-H.; Chang, G.-F.; Kumar, A.; Lin, G.-F.; Luo, L.-Y.; Chinga, E. W.-G. D. *Chem. Commun.* **2008**, 978−980. (c) Chang, G.-F.; Kumar, A.; Ching, W.-M.; Chu, H.-W.; Hung, C.-H. *Chem.—Asian. J.* **2009**, *4*, 164−173.

(14) (a) Matano, Y.; Miyajima, T.; Nakabuchi, T.; Imahori, H.; Ochi, Y.; Sakaki, S. *J. Am. Chem. Soc.* **2006**, *128*, 11760−11761. (b) Ochi, N.; Nakao, Y.; Sato, H.; Matano, Y.; Imahori, H.; Sakaki, S. *J. Am. Chem. Soc.* **2009**, *131*, 10955−10963. (c) Matano, Y.; Miyajima, T.; Ochi, N.; Nakao, Y.; Sakaki, S.; Imahori, H. *J. Org. Chem.* **2008**, *73*, 5139−5142.

(15) Skonieczny, J.; Latos-Grażyński, L.; Szterenberg, L. *Org. Biomol. Chem.* **2012**, *10*, 3463−3471.

(16) (a) Zeng, Q.; Li, Z.; Dong, Y.; Di, C.; Qin, A.; Hong, Y.; Ji, L.; Zhu, Z.; Jim, C. K. W.; Yu, G.; Li, Q.; Li, Z.; Liu, Y.; Qin, J.; Tang, B. Z. *Chem. Commun.* **2007**, 70−72. (b) Hong, Y.; Lama, J. W. Y.; Tang, B. Z. *Chem. Commun.* **2009**, 4332−4353. (c) Yuan, W. Z.; Lu, P.; Chen, S.; Lam, J. W. Y.; Wang, Z.; Liu, Y.; Kwok, H. S.; Ma, Y.; Tang, B. Z. *Adv. Mater.* **2010**, *22*, 2159−2163. (d) Salini, P. S.; Holaday, M. G. D.; Reddy, M. L. P.; Suresh, C. H.; Srinivasan, A. *Chem. Commun.* **2013**, *49*, 2213−2215.

(17) (a) Jang, Y.-S.; Kim, H.-J.; Lee, P.-H.; Lee, C. H. *Tetrahedron Lett.* **2000**, *41*, 2919−2923. (b) Won, D. H.; Lee, C. H. *Tetrahedron Lett.* **2003**, *44*, 6695−6697.

(18) Sessler, J. L.; An, D.; Cho, W.-S.; Lynch, V.; Yoon, D.-W.; Hong, S.-J.; Lee, C.-H. *J. Org. Chem.* **2005**, *70*, 1511−1517.

(19) Sridevi, B.; Narayanan, S. J.; Rao, R.; Chandrashekar, T. K.; Englich, U.; Senge, K. R. *Inorg. Chem.* **2000**, *39*, 3669−3677.

(20) Benesi, H. A.; Hildebrand, J. H. *J. Am. Chem. Soc.* **1949**, *71*, 2703−2705.

(21) (a) Kumar, M. R.; Chandrashekar, T. K. *J. Inclusion Phenom. Macrocyclic Chem.* **1999**, *35*, 553−582. (b) Anand, V. G.; Pushpan, S. K.; Venkatraman, S.; Dey, A.; Chandrashekar, T. K.; Joshi, B. S.; Roy, R.; Teng, W.; Senge, K. R. *J. Am. Chem. Soc.* **2001**, *123*, 8620−8621.